Band alignment of ZnO-based nanorod arrays for enhanced visible light photocatalytic performance

Jing Wan,[1] Aseel Shaker Al-Baldawy,[2] Shanzhi Qu,[1] Jinshen Lan,[1] Xiaofang Ye,[1] Yuchen Fei,[1] Jingtian Zhao,[1] Ziyun Wang,[1] Rongdun Hong,[1] Shengshi Guo,[1] Shengli Huang,[1]* Shuping Li,[1]* Junyong Kang[1]

[1]Engineering Research Center of Micro-nano Optoelectronic Materials and Devices, Ministry of Education, Fujian Key Laboratory of Semiconductor Materialsand Applications, CI Center for OSED, Department of Physics, Jiujiang Research Institute, Xiamen University, Xiamen 361005, China

[2]Department of Food Science, Faculty of Agriculture, University of Kufa, Kufa, Najaf 054003, Iraq

*Corresponding authors, E-mail: huangsl@xmu.edu.cn (S. Huang) and lsp@xmu.edu.cn (S. Li).

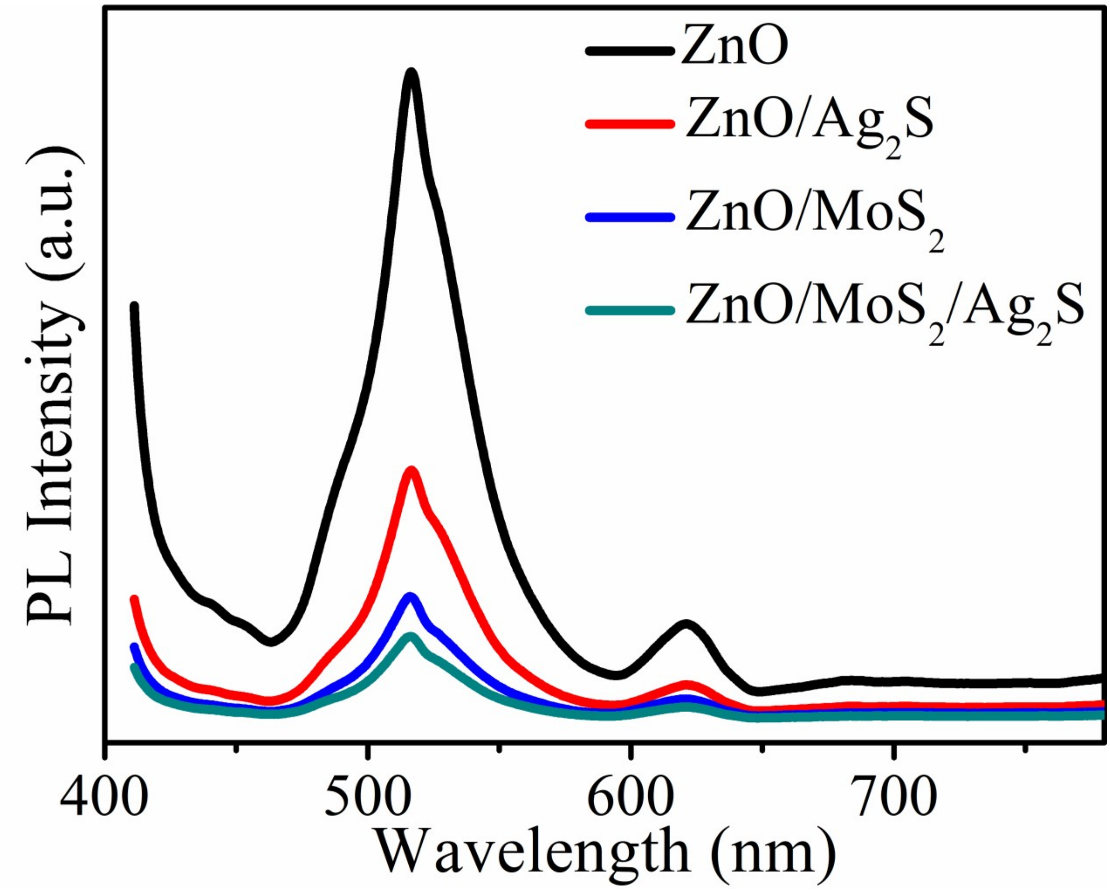

Figure S1. PL spectra of the specimens at the excitation wavelength of 400 nm.

Figure S1 presents PL spectra of the samples at the excitation wavelength of 400 nm. Three peaks at 515, 530 and 621 nm are observed for all the specimens. Comparing with the PL spectra at the excitation wavelength of 325 nm in Fig. 4(b), the bandedge emission disappears and the fluorescence emissions red shit as the excitation wavelength increases. Moreover, the peak intensity decreases successively in the order of ZnO, ZnO/Ag_2S, ZnO/MoS_2, and $ZnO/MoS_2/Ag_2S$. The red-shit of the fluorescence emissions is due to the reduced excitation energy, as those found in literature [1]. The decreasing emission suggests limited exciton recombination in the heterogeneous specimens and is advantageous for the photocatalytic performance.

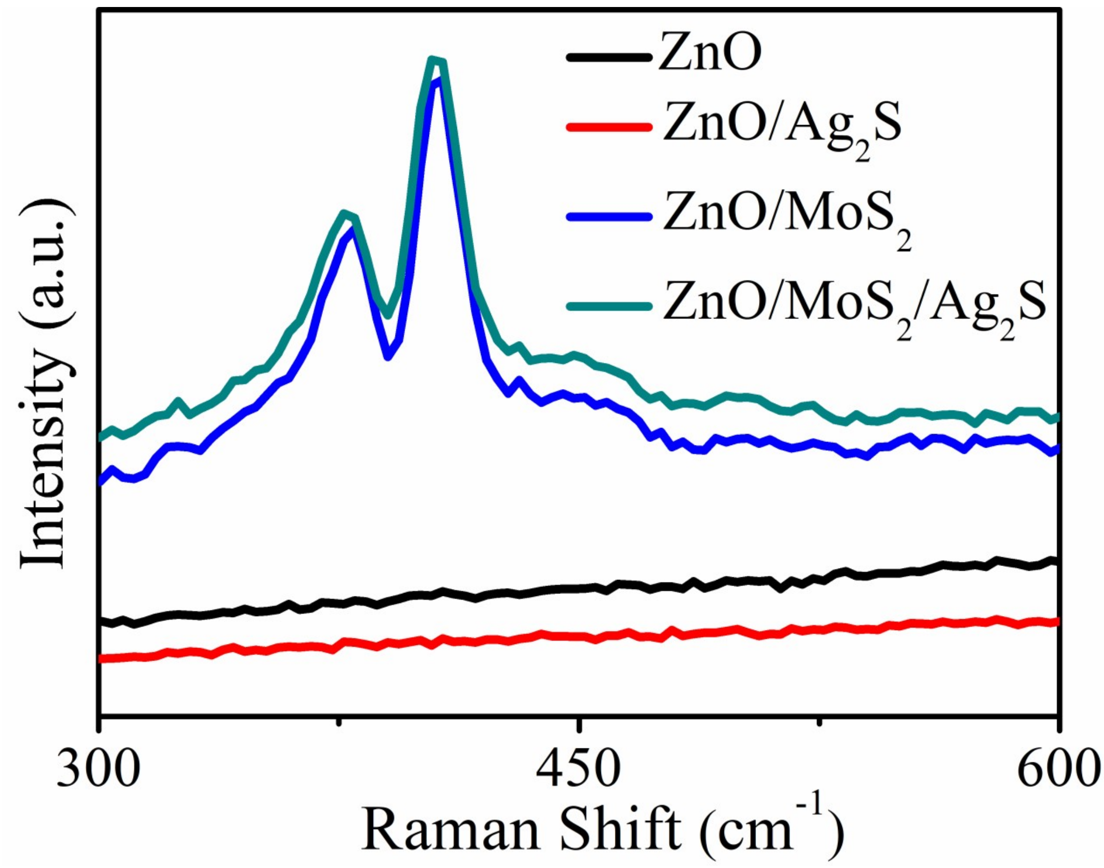

Figure S2. Raman spectra of the specimens.

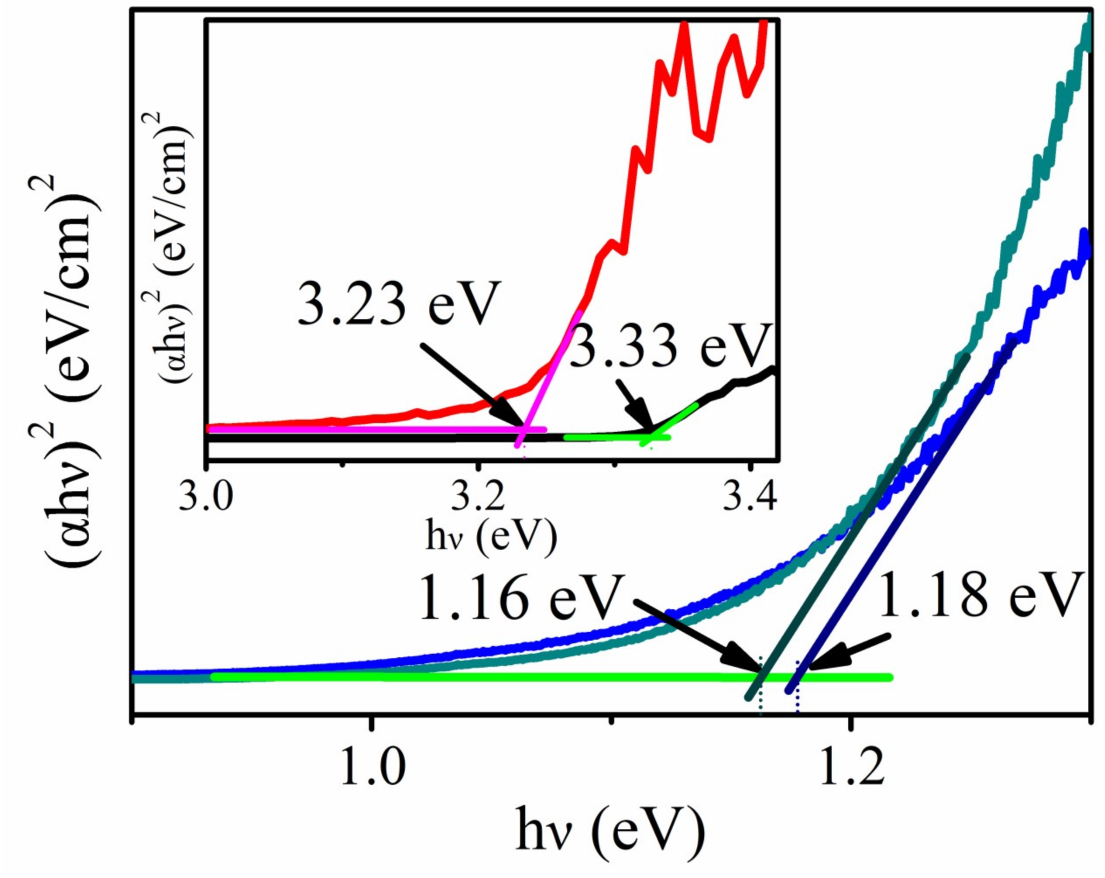

Figure S3. Tauc plots of absorption spectra of the specimens.

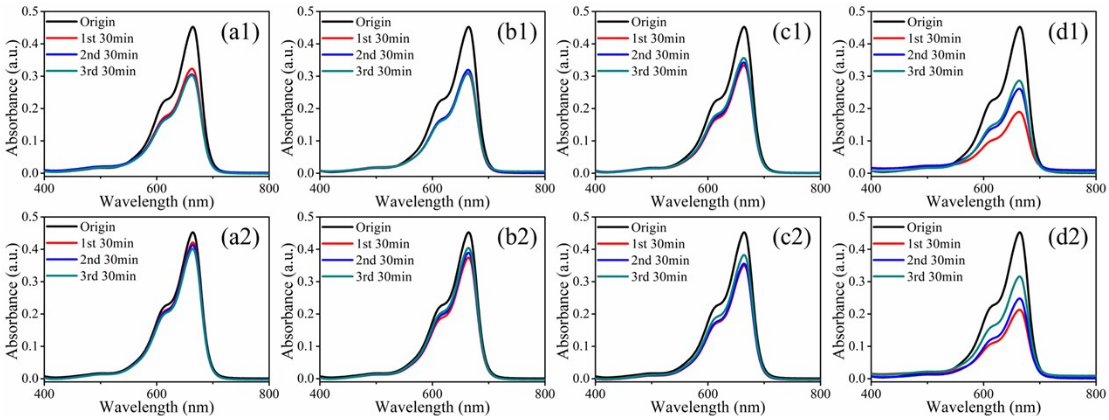

Figure S4. Absorption spectra of degraded MB aqueous solutions as catalyzed by ZnO nanowire arrays with different coating layer under (a1-d1) UV light and (a2-d2) visible light for different periods: (a1,a2) ZnO, (b1,b2) ZnO/Ag_2S, (c1,c2) ZnO/MoS_2, (d1,d2) ZnO/MoS_2/Ag_2S.

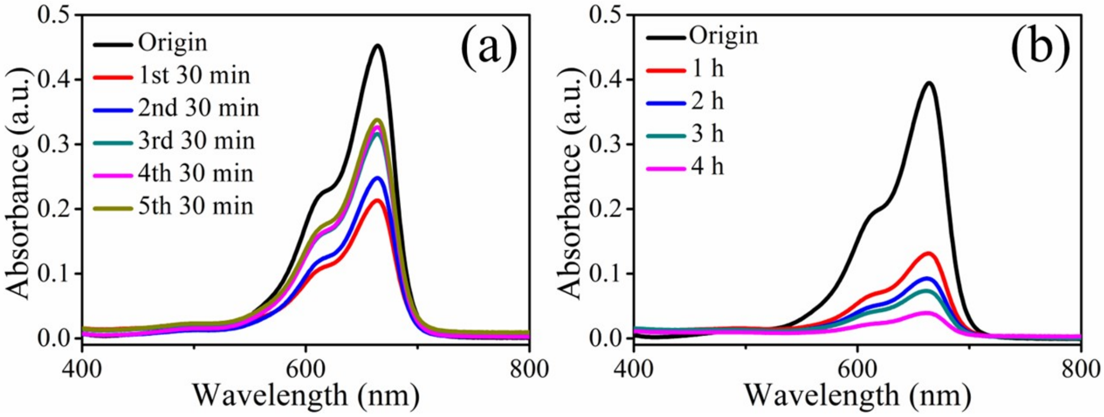

Figure S5. Absorption spectra of the degraded MB aqueous solution as catalyzed by ZnO/MoS_2/Ag_2S array under visible light in different conditions: (a) a specimen in 5 successive periods, (b) 4 specimens in each period.

Figure S5(a) demonstrates degradation of MB solution as catalyzed by ZnO/MoS_2/Ag_2S array at different cycles under visible light. The degradation efficiency obtained from the figure is listed in Table S2. It can be seen that the efficiency decreases in the first three cycles but nearly keeps stable after 3 cycles. However, even in the 5th cycle, the efficiency of 25.30% is also larger than that of other samples in the 1st cycle under visible light, indicating a good photocatalytic stability of $ZnO/MoS_2/Ag_2S$ array. Figure S5(b) displays the degradation of MB aqueous solution as catalyzed by $ZnO/MoS_2/Ag_2S$ arrays in different time length under visible light. The band intensity decreases with extending the photocatalytic time, suggesting an increasing degradation efficiency. The efficiency obtained from the figure is also listed in Table S2. The efficiency increases with extending period and reaches 90.09% in 4 h. From the variation tendency, it can be speculated that the MB dye might be degraded completely in about 5.5 h.

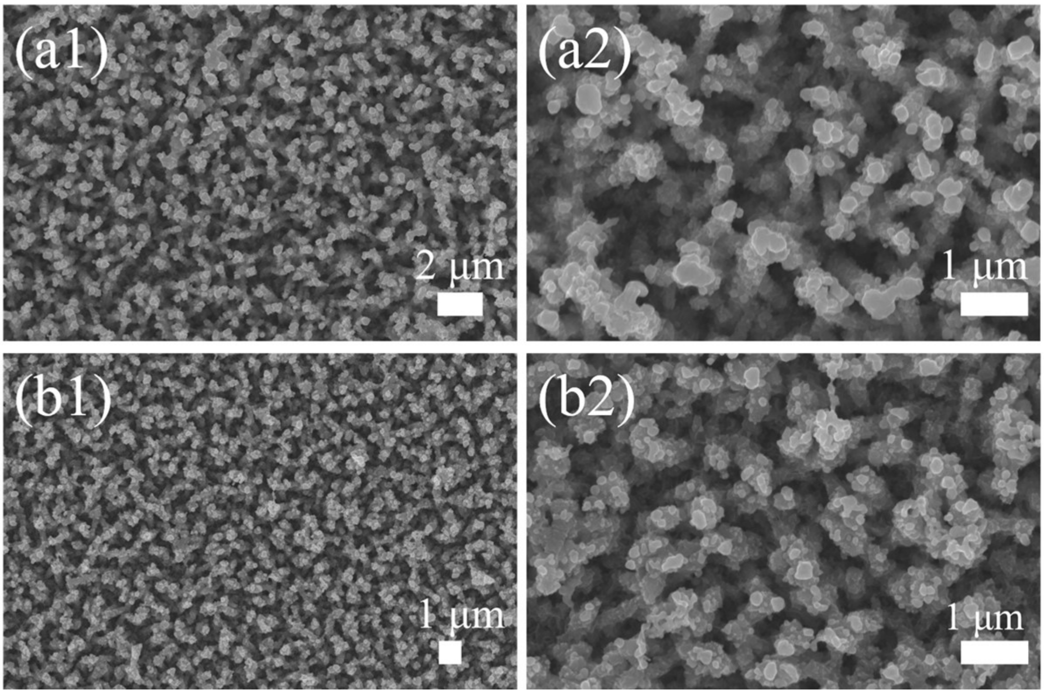

Figure S6. SEM images of $ZnO/MoS_2/Ag_2S$ array: (a1,a2) before photocatalysis, (b1,b2) after photocatalysis for 5 cycles.

SEM images of $ZnO/MoS_2/Ag_2S$ array before and after 5-cycle photocatalysis were tested and supplied in Fig. S6. It is found that the nanorod array remains normal to the substrate after photocatalysis. There is not clear difference in the array structure before and after photocatalytic performance. This indicates that the nanorod array possesses a good structural stability for the photocatalysis.

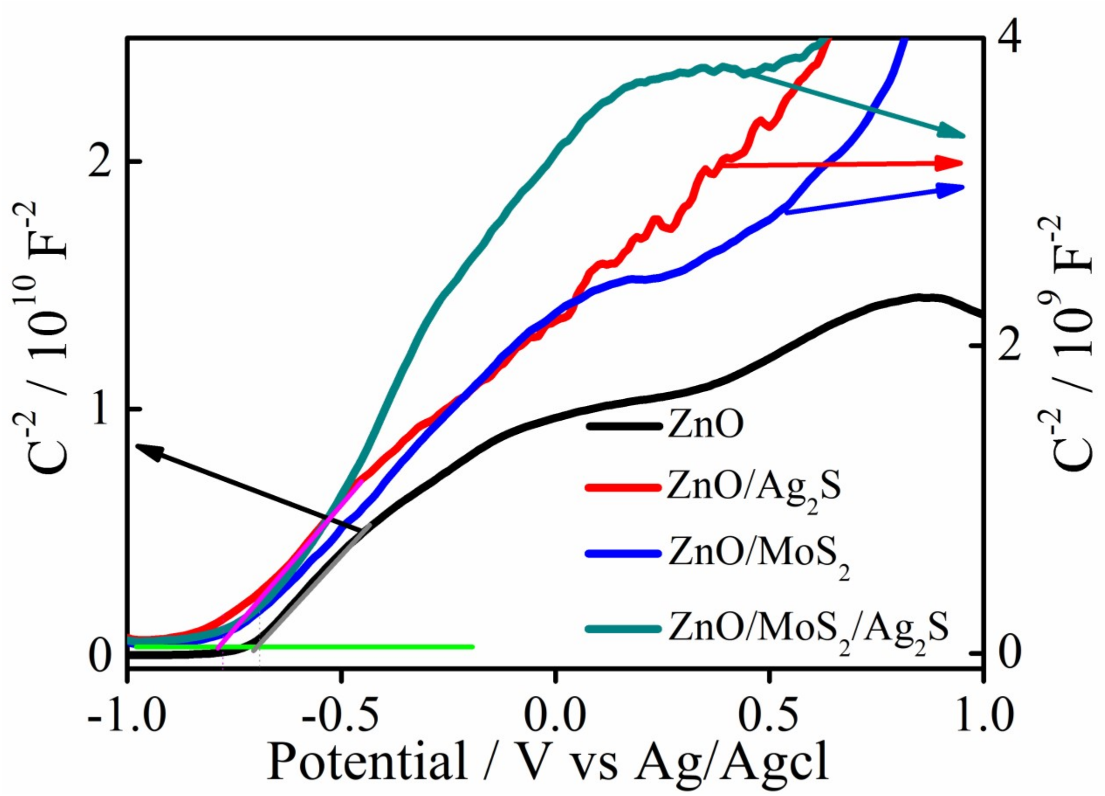

Figure S7. Mott−Schottky plots of the specimens.

To gain deep insight of the photocatalytic activity, energy band diagrams of the specimens were depicted by measuring Mott−Schottky (MS) curves in the dark at an AC frequency of 1.0 kHz, as shown in Fig. S7. By extrapolating the X-intercept of the linear region in the MS plots at Y = 0, the flat band potential (E_{FB}) of ZnO and Ag_2S is achieved, which can be converted to the normal hydrogen electrode potential (E_{NHE}) according to the Nernst equation [2],

$$E_{NHE} = E_{FB} + E^{0}_{Ag/Agcl}, \quad (1)$$

where $E^{0}_{Ag/Agcl} = 0.197$ eV at room temperature. Combing the values of E_{NHE} and Eg as achieved in Fig. S2, the conduction band minimum (E_{CBM}) and valence band maximum (E_{VBM}) relative to the vacuum potential can be roughly estimated by the following equations,

$$E_{CBM} = -E_{NHE} - 4.5, \quad (2)$$

$$E_{VBM} = -E_{NHE} - 4.5 - Eg. \quad (3)$$

Therefore, the CB of ZnO and Ag_2S can be calculated to be -4.00 eV and -3.90 eV, respectively from the MS plots.

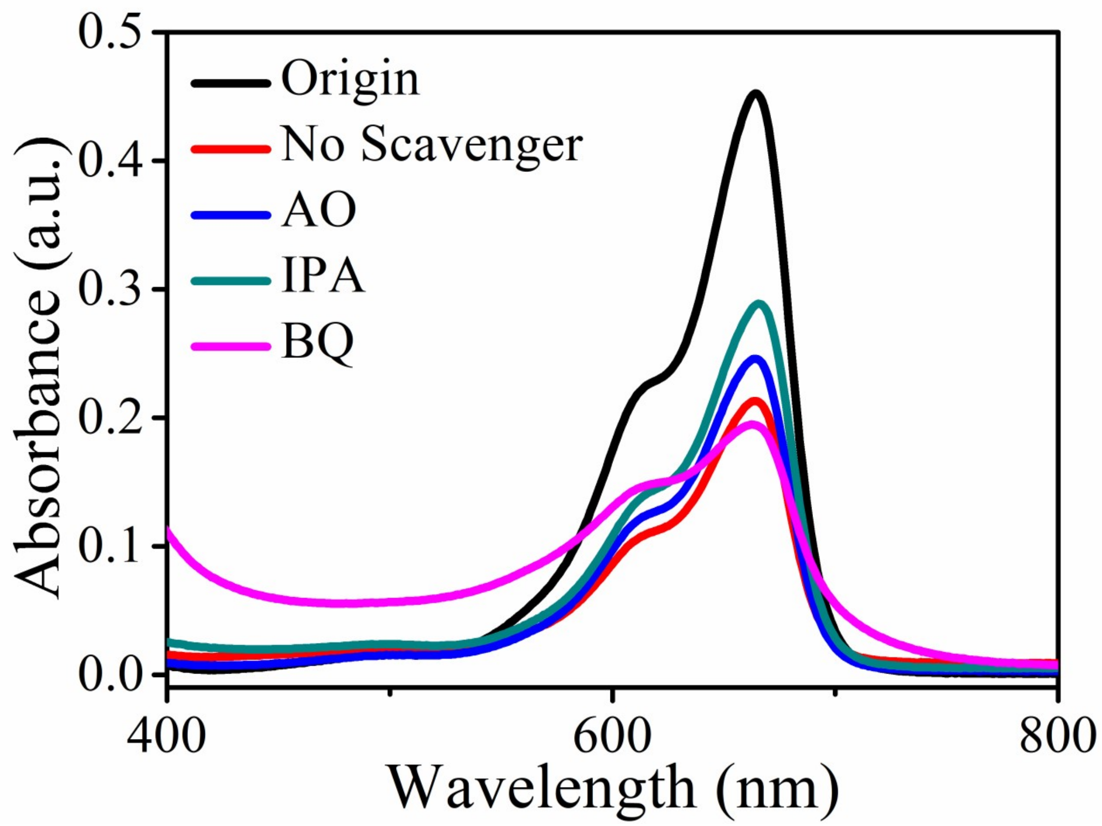

Figure S8. Absorption spectra of the degraded MB solution as catalyzed by $ZnO/MoS_2/Ag_2S$ nanoarrays under visible light irradiation for 30 min with different scavengers.

For free radical trapping experiments, isopropanol (IPA) was used as ·OH scavenger, benzoquinone (BQ) as $O_2^{\cdot-}$ scavenger, and ammonium oxalate (AO) as h^+ scavenger [3]. The scavengers were added into the MB solutions with identical concentration initially and individually. Afterward, the solution and the catalyst were subjected to the simulated sunlight for 30 min. Figure S8 presents absorption spectra of the degraded solution, in which the degradation efficiency is calculated and supplied in Table S4. After adding IPA, the degradation efficiency decreases significantly from 52.88% to 36.17%. When IPA is replaced by AO, the degradation efficiency drops to 45.63%. However the degradation efficiency reaches 55.80% when BQ is in the solution, which is close to the efficiency without scavenger. Therefore, the BQ is ineffective on the degradation of MB. These results suggest that the $O_2^{\cdot -}$ radicals don't work in the photodegradation, while the ·OH and h^+ radicals play an important role in it, especially for the ·OH radicals.

Table S1. Photodegradation efficiency of MB solution as achieved in Fig. S4.

Light irrediation	Time	ZnO	ZnO/Ag_2S	ZnO/MoS_2	$ZnO/MoS_2/Ag_2S$
UV	1^{st} 30 min	28.55%	31.91%	26.28%	58.12%
	2^{nd} 30 min	32.40%	29.30%	24.33%	42.32%
	3^{rd} 30 min	33.11%	31.38%	21.22%	36.79%
Visible	1^{st} 30 min	6.94%	17.24%	22.74%	52.88%
	2^{nd} 30 min	8.69%	14.01%	21.39%	45.19%
	3^{rd} 30 min	11.27%	10.67%	15.49%	30.17%

Table S2. Photodegradation efficiencies of MB solution as achieved in Fig. S5.

Period	1st 30 min	2nd 30 min	3rd 30 min	4th 30 min	5th 30 min
Efficiency	52.88%	45.19%	30.17%	27.85%	25.30%
Period	1 h	2 h	3 h	4 h	/
Efficiency	66.77%	76.58%	81.45%	90.09%	/

Table S3. Comparison of photocatalytic efficiency of $ZnO/MoS_2/Ag_2S$ nanorod array and other catalysts in literature.

Catalyst	Pollutant	Pollutant concentration	Active area (cm^2)	Volume (mL)	Degradation efficiency (%)	Time (min)	Ref.
ZnO/Si	MB	1×10^{-5} M	1×1.5	20	15.26	60	[4]
$ZnO/Si/Ag_2S$	MB	5×10^{-6} M	1×1	5	62	60	[5]
$ZnO/SnO_2/Ag_2S$	MB	5×10^{-6} M	1×1	5	71.61	60	[6]
ZnO/CdS	EBT	10 mg/L	1×1	30	42	90	[7]
$TiO_2/SnS_2/MoS_2$	MB	5 mg/L	1×2	10	81.8	90	[8]
ZnO/Bi_2S_3	TBBPA	10 mg/L	2×4	50	60.9	30	[9]
Ag-CoAl-LDH/TiO_2	LVFX	10 mg/L	2×2	10	95.2	120	[10]
$ZnO/MoS_2/Ag_2S$	MB	5×10^{-6} M	1×2	5	52.88	30	This work

Table S4. Degradation efficiency of MB solution with different scavengers as calculated from Fig. S8.

	No Scavenger	AO	IPA	BQ
Efficiency	52.88%	45.63%	36.17%	55.80%

References

[1] Bingjie Yu, Yunpeng Liu, Mengmeng Cao, Mengmeng Zhu, Renjie Chen and Huili Li, Multi-color carbon dots from cis-butenedioic acid and urea and highly luminescent carbon dots@$Ca(OH)_2$ hybrid phosphors with excellent thermal stability for white light-emitting diodes, J. Lumin. 2021, 237, 118202.

[2] Mitra Mousavi, Mohammad Mehdi Habibi, Gaoke Zhang, Pouran Pourhakkak, Sahar moradian and Jahan B. Ghasemi, In-situ construction of ZnO/Sb_2MoO_6 nano-heterostructure for efficient visible-light photocatalytic conversion of N_2 to NH_3, Surf. Interfaces 2022, 30, 101844.

[3] Ni Huang, Jinxia Shu, Zhonghua Wang, Ming Chen, Chunguang Ren and Wei Zhang, One-step pyrolytic synthesis of ZnO nanorods with enhanced photocatalytic activity and high photostability under visible light and UV light irradiation, J. Alloy. Compd, 2015, 648, 919-929.

[4] Dingguo Li, Xiaolan Yan, Chunhua Lin, Shengli Huang, Z. Ryan Tian, Bing He, Qianqian Yang, Binbin Yu, Xu He, Jing Li, Jiayuan Wang, Huahan Zhan, Shuping Li and Junyong Kang, Synthesis of ZnO/Si Hierarchical Nanowire Arrays for Photocatalyst Application, Nanoscale Res. Lett. 2017, 12, 10.

[5] Jinshen Lan, Bing He, Choonyian Haw, Mengyao Gao, Imran Khana, Rongsheng Zheng, Shengshi Guo, Jingtian Zhao, Ziyun Wang, Shengli Huanga, Shuping Li and Junyong Kang, Band engineering of ZnO/Si nanowire arrays in Z-scheme heterojunction for efficient dye photodegradation, Appl. Surf. Sci. 2020, 529, 147203.

[6] Jinshen Lan, Mengyao Gao, Choonyian Haw, Imran Khan, Jingtian Zhao, Ziyun Wang, Shengshi Guo, Shengli Huang, Shuping Li, Junyong Kang, Layer-by-layer assembly of Ag_2S quantum dots-sensitized ZnO/SnO_2 core-shell nanowire arrays for enhanced photocatalytic activity, Phys. Lett. A 2020, 384, 126708.

[7] Chunmei Li, Taha Ahmed, Mingguo Ma, Tomas Edvinsson, Jiefang Zhu, A facile approach to ZnO/CdS nanoarrays and their photocatalytic and photoelectrochemical properties, Appl. Catal. B-Environ. 2013, 138-139, 175-183.

[8] Juan Gao, Jintao Hu, Yanfen Wang, Lingcheng Zheng, Gang He, Jiale Deng, Mei Liu, Yang Li, Yin Liu, Hongli Zhou, Fabrication of Z-scheme $TiO_2/SnS_2/MoS_2$ ternary heterojunction arrays for enhanced photocatalytic and photoelectrochemical performance under visible light, J. Solid State Chem. 2022, 307, 122737.

[9] Xianglin Sun, Hao Wu, Yiming Tang, Zexiao Zheng, Yaping Li, Laisheng Li, Qiuyun Zhang, Enhanced photoelectrocatalytic degradation of tetrabromobisphenol a from tip-decorated ZnO nanorod electrode with Bi_2S_3 nanoparticles, Mat. Sci. Semicon. Proc. 2021, 128, 105724.

[10] Chunsheng Ding, Jun Guo, Wei Gan, Peng Chen, Ziliang Li, Zhuangzhuang Yin, Shihan Qi, Shangkun Deng, Miao Zhang, Zhaoqi Sun, Ag nanoparticles decorated Z-scheme CoAl-LDH/TiO_2 heterojunction photocatalyst for expeditious levofloxacin degradation and Cr(VI) reduction, Sep. Purif. Technol. 2022, 297, 121480.